Ruthenium complexes of chiral diphosphinite ligands with cyclohexane or *chiro* -inositol backbones as catalysts for asymmetric hydrogenation reactions

George R. Clark[a]; Andrew Falshaw[b]; Graeme J. Gainsford[b]; Cornelis Lensink[b]; Angela T. Slade[a]; L. James Wright[a]

[a] Department of Chemistry, The University of Auckland, Auckland, New Zealand [b] Industrial Research Limited, Lower Hutt, New Zealand

PLEASE SCROLL DOWN FOR ARTICLE

Taylor & Francis
Taylor & Francis Group

Ruthenium complexes of chiral diphosphinite ligands with cyclohexane or *chiro*-inositol backbones as catalysts for asymmetric hydrogenation reactions

GEORGE R. CLARK†, ANDREW FALSHAW‡, GRAEME J. GAINSFORD‡,
CORNELIS LENSINK‡, ANGELA T. SLADE† and L. JAMES WRIGHT*†

†Department of Chemistry, The University of Auckland, Private Bag 92019,
Auckland, New Zealand
‡Industrial Research Limited, PO Box 31-310, Lower Hutt, New Zealand

Treatment of $[RuCl_2(COD)]_n$ with the chiral diphosphinite ligand (1*S*,2*S*)-1,2-*trans*-bis-(*O*-diphenylphosphino)cyclohexane [(1*S*,2*S*)-**14**] and triethylamine gives the bis(diphosphinite) complex $RuHCl[(1S,2S)$-**14**$]_2$ (**15**) in good yield. If (*rac*)-1,2-*trans*-bis-(*O*-diphenylphosphino)-cyclohexane [(*rac*)-**14**] is used in place of (1*S*,2*S*)-**14** in this reaction, a racemic mixture of $RuHCl[(1S,2S)$-**14**$]_2$ and $RuHCl[(1R,2R)$-**14**$]_2$ [(*rac*)-**16**] is formed. The X-ray crystal structure of (*rac*)-**16**·(2.5CH_2Cl_2) has been determined. Treatment of (*rac*)-**16** with hydrogen in iso-propanol leads to the formation of a racemic mixture of $RuH_2[(1S,2S)$-**14**$]_2$ and $RuH_2[(1R,2R)$-**14**$]_2$ [(*rac*)-**17**]. The structure of (*rac*)-**17** was confirmed by the X-ray analysis of a racemic crystal. Ruthenium mono(diphosphinite), diamine complexes of the general formula $RuCl_2(NN)(PP)$ are formed by the treatment of $RuCl_2(PPh_3)_3$ with the appropriate diphosphinite (PP) and diamine (NN) ligands. In this way, the following complexes have been synthesized: $RuCl_2[(+)$-DPEN$][(1S,2S)$-**14**] (**18**), $RuCl_2[(−)$-DPEN$][(1S,2S)$-**14**] (**19**), $RuCl_2[(+)$-DPEN$][(1R,2R)$-**14**] (**20**), $RuCl_2[(−)$-DPEN$][(1R,2R)$-**14**] (**21**), $RuCl_2[(+)$-DPEN$][(rac)$-**14**] (**22**), $RuCl_2[(−)$-DPEN$][(rac)$-**14**] (**23**), $RuCl_2(D$-NN2$)[(1S,2S)$-**14**] (**24**), $RuCl_2(EDA)[(1S,2S)$-**14**] (**25**), $RuCl_2(D$-NN2$)(D$-10$)$ (**26**), $RuCl_2(EDA)(D$-10$)$ (**27**), $RuCl_2[(+)$-DPEN$](D$-10Et$)$ (**28**), $RuCl_2(D$-NN2$)(D$-10Et$)$ (**29**), [where DPEN = 1,2-diphenylethylenediamine, D-NN2 = 1D-1,2-dideoxy-1,2-diamino-3,4,5,6-tetra-*O*-benzyl-*myo*-inositol, EDA = 1,2-diaminoethane, D-10 = 1D-3,4-bis(*O*-diphenylphosphino)-1,2,5,6-tetra-*O*-methyl-*chiro*-inositol, D-10Et = 1D-3,4-bis(*O*-diphenylphosphino)-1,2,5,6-tetra-*O*-ethyl-*chiro*-inositol]. These ruthenium complexes catalyze the hydrogenation of the ketones acetophenone and 3-quinuclidinone to give the corresponding alcohols in high yields, but with moderate to low enantiomeric excesses.

Keywords: Ruthenium; Catalytic asymmetric hydrogenation of ketones; *Chiro*-inositol; Chiral diphosphinite ligand; X-ray crystal structure

1. Introduction

A large number of studies have focused on the development of chiral ligands for transition metal catalyzed asymmetric transformations of prochiral substrates [1].

*Corresponding author. Email: lj.wright@auckland.ac.nz

A general observation is that catalysts incorporating a given chiral ligand do not form products of high enantiomeric purity with all prochiral substrates, and this has provided a major impetus for the development of new chiral ligands [2]. Phosphorus donors have been most commonly employed in the design of new chiral ligands [2, 3], and we recently reported our preliminary results of the synthesis and study of new chiral diphosphinite ligands that incorporate a *chiro*-inositol backbone [4]. Attractive features of *chiro*-inositol (figure 1) that are not shared with many other carbohydrates are the chemically robust cyclohexane backbone, the ready availability of both the D- and
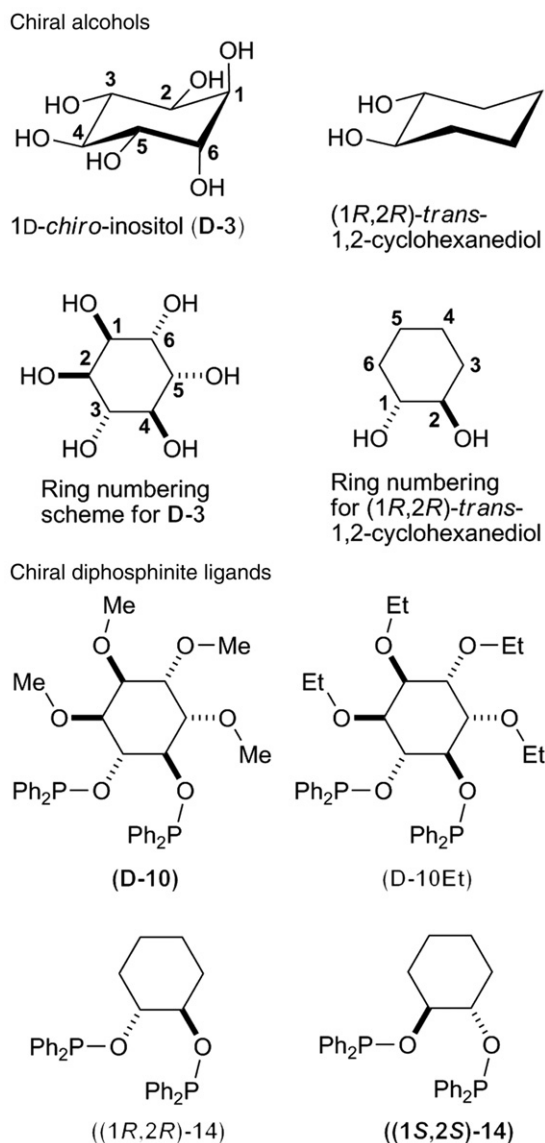

Figure 1.   Chiral alcohols and the chiral diphosphinite ligands synthesized from these.

L-enantiomers from natural products, and the presence of six hydroxyl groups that provide extensive scope for selective functionalization. Although a number of chiral, phosphorus-donor ligands based on other carbohydrates have been synthesized for transition-metal-catalyzed asymmetric transformations [5–11], chiral inositols have been rarely studied in this context [12]. In our recent study, we found that ruthenium derivatives of *chiro*-inositol-based diphosphinite ligand, D-10 (figure 1), catalyze the asymmetric hydrogenation of some ketones to give products with low to moderate enantiomeric excesses. In an extension of this work, we have investigated the catalytic activities of a series of ruthenium complexes that contain related diphosphinite ligands in which the four remote carbon centers in the cyclohexane rings bear different substituents. Chiral diamine ligands have also been incorporated into some of these complexes as these ligands have been shown, in some cases, to enhance the enantioselectivity of asymmetric hydrogenation reactions [13]. We now report (1) the synthesis of the chiral ruthenium diphosphinite complexes **15–29** (schemes 2 and 3); (2) the crystal structures of a racemic mixture of RuHCl[(1*S*,2*S*)-14]$_2$ and RuHCl[(1*R*,2*R*)-14]$_2$ [(*rac*)-**16**] and a racemic mixture of RuH$_2$[(1*S*,2*S*)-14]$_2$ and RuH$_2$[(1*R*,2*R*)-14]$_2$ [(*rac*)-**17**] [(1*S*,2*S*)-**14**] = (1*S*,2*S*)-1,2-*trans*-bis-(*O*-diphenylphosphino)cyclohexane; and (3) the results of catalytic asymmetric hydrogenation studies of the prochiral ketones acetophenone and 3-quinuclidinone in the presence of **15–29**.

2. Results and discussion

2.1. *The chiral diphosphinite ligands, 1D-3,4-bis(O-diphenylphosphino)-1,2,5, 6-tetra-O-methyl-chiro-inositol (D-10), 1D-3,4-bis(O-diphenylphosphino)-1,2,5, 6-tetra-O-ethyl-chiro-inositol (D-10Et), (1R,2R)-1,2-trans-bis-(O-diphenyl-phosphino)cyclohexane [(1R,2R)-14], (1S,2S)-14, and (rac)-14*

We have previously reported the synthesis of the *chiro*-inositol-derived diphosphinite ligand 1D-3,4-bis(*O*-diphenylphosphino)-1,2,5,6-tetra-*O*-methyl-*chiro*-inositol (D-10) [4]. The more sterically encumbered analogue, 1D-3,4-bis(*O*-diphenylphosphino)-1,2,5,6-tetra-*O*-ethyl-*chiro*-inositol (D-10Et) (see figure 1), can be prepared in a parallel manner, but with the alkylating agent EtBr replacing the MeI used in the original synthetic sequence, as indicated in scheme 1. For the clarity and ease of comparison, the same compound numbering scheme that was used in our previous report [4] is also used in this article, and the numbering of new compounds in this article continues on from this original numbering scheme. Spectroscopic data for D-10Et and all other new compounds reported in this article are collected in section 3. The NMR spectral data for D-10Et are consistent with the C_2 symmetry of the molecule. Thus, in the ^{1}H NMR spectrum, two apparent triplet signals at 0.64 and 1.18 ppm are observed for the CH$_3$ groups of the two sets of symmetry-related ethyl groups. Complex sets of overlapping signals are observed for the CH and CH$_2$ resonances in the region 2.72–4.93 ppm. In the ^{13}C NMR spectrum, resonances for the methyl groups are observed at 14.7 and 15.4 ppm, and resonances at 66.9 and 67.2 ppm are observed for the methylene groups. The three pairs of CH signals are observed at 76.1, 77.9, and 78.9 ppm. In the ^{31}P NMR spectrum of D-10Et, a singlet at 109.47 ppm is observed for the two equivalent phosphorus atoms.
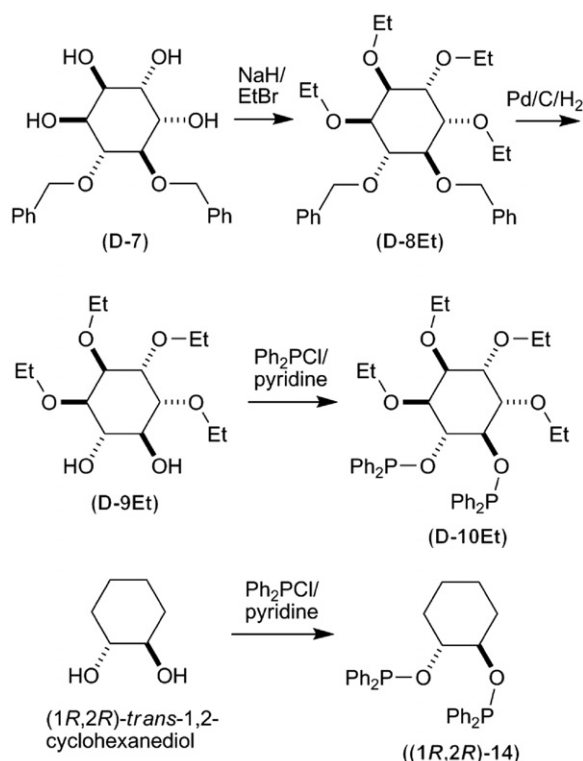
Scheme 1.   Syntheses of the chiral ligands D-10Et and (1*R*,2*R*)-**14**.

The previously reported chiral diphosphinite ligands (1*R*,2*R*)-1,2-*trans*-bis-(*O*-diphenylphosphino)cyclohexane [(1*R*,2*R*)-14] [14] and (1*S*,2*S*)-1,2-*trans*-bis-(*O*-diphenylphosphino)cyclohexane [(1*S*,2*S*)-**14**] [15], as well as the racemic mixture of these two chiral ligands, [(*rac*)-**14**] (see figure 1), were prepared from the corresponding alcohols by treating with Ph₂PCl, using a slightly modified version of the literature procedure (see scheme 1 and section 3).

2.2. *Synthesis of the bis(diphosphinite) complexes RuHCl[(1S,2S)-14]₂ (15), a racemic mixture of 15 and RuHCl[(1R,2R)-14]₂ [(rac)-16], and a racemic mixture of RuH₂[(1S,2S)-14]₂ and RuH₂[(1R,2R)-14]₂ [(rac)-17]*

Complexes containing chiral diphosphinite ligands that have the general formula $R_2PO-X-OPR_2$ (where X is a chiral bridging group) are well known for a number of metals, including rhodium [16]. However, ruthenium derivatives of ligands of this type are relatively rare [17, 18]. In an extension of our previous study, in which we reported that treatment of $[RuCl_2(COD)]_n$ with D-10 in the presence of triethylamine [19] gives RuHCl(D-10)₂ (**11**), we now report that the treatment of $[RuCl_2(COD)]_n$ with (1*S*,2*S*)-**14** and triethylamine gives the closely related orange/yellow bis(diphosphinite) complex, RuHCl((1*S*,2*S*)-14)₂ (**15**) (scheme 2). The hydride ligand in **15** probably originates from the β-hydride elimination of coordinated triethylamine in an intermediate complex [19d]. The NMR spectroscopic data for **15** are consistent with the idealized geometry
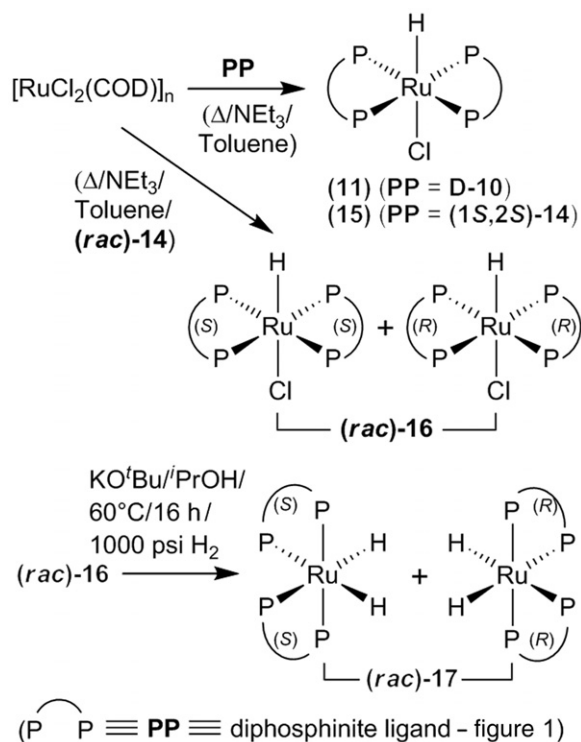
Scheme 2. Syntheses of **11**, **15**, (*rac*)-**16**, and (*rac*)-**17**.

drawn in scheme 2 and a single crystal X-ray structure determination of (*rac*)-**16** reveals that this overall geometry is retained in the solid state. Although the C_2 axis of the free diphosphinite ligand, (1*S*,2*S*)-**14** is no longer present in **15**. In the idealized structure drawn in scheme 2 there is a C_2 axis that passes through H, Ru, and Cl. Thus, the two phosphorus atoms and the six cyclohexane ring carbons within one diphosphinite ligand are all inequivalent, but each of these atoms is related by the C_2 axis to a corresponding atom in the other ligand. Consequently, six signals are observed for the cyclohexane ring carbons in the ^{13}C NMR spectrum of **15** (at 24.4, 24.5, 32.3, 33.0, 75.7, and 78.9 ppm). In the ^{31}P NMR spectrum two apparent triplets are observed for each symmetry-related pair of phosphorus atoms (at 118.13 and 147.26 ppm), consistent with coupling in the AA′XX′ spin system [20]. In the ^{1}H NMR spectrum of **15** two multiplets that each integrate for two protons at 3.76 and 5.10 ppm are observed for the two pairs of cyclohexane CH protons, and a complex set of overlapping multiplets in the region 0.80–2.35 ppm is observed for the CH$_2$ groups. The hydride resonance is observed as a multiplet at −16.38 ppm. In the solid state, **15** survives unchanged on exposure to air for months, although in solution compound **15** is slowly degraded by atmospheric oxygen over a period of hours.

If (1*S*,2*S*)-**14**, that is used in the synthesis of **15**, is replaced with [(*rac*)-**14**], the product formed is a racemic mixture of the two complexes RuHCl[(1*S*,2*S*)-14]$_2$ and RuHCl[(1*R*,2*R*)-14]$_2$ [(*rac*)-**16**]. The spectral data for (*rac*)-**16** is identical to that observed for **15**. A crystal of (*rac*)-**16** suitable for X-ray structure determination was

$$RuCl_2(PPh_3)_3 + PP + NN \xrightarrow{\text{Toluene/}\atop\text{RT/2 hrs}}$$

	PP	NN
(12)	(D-10;	(+)-DPEN)
(13)	(D-10;	(-)-DPEN)
(18)	((1S,2S)-**14**;	(+)-DPEN)
(19)	((1S,2S)-**14**;	(-)-DPEN)
(20)	((1R,2R)-**14**;	(+)-DPEN)
(21)	((1R,2R)-**14**;	(-)-DPEN)
(22)	((1R,2R)-**14**);	(+)-DPEN
	& ((1S,2S)-**14**;	(+)-DPEN)
(23)	((1R,2R)-**14**);	(-)-DPEN
	& ((1S,2S)-**14**;	(-)-DPEN)
(24)	((1S,2S)-**14**;	D-NN2)
(25)	((1S,2S)-**14**;	EDA)
(26)	(D-10;	D-NN2)
(27)	(D-10;	EDA)
(28)	(D-10Et;	(+)-DPEN)
(29)	(D-10Et;	D-NN2)

(P⌒P ≡ PP ≡ diphosphinite ligand – figure 1)

(N⌒N ≡ NN ≡ diamine ligand – figure 4)
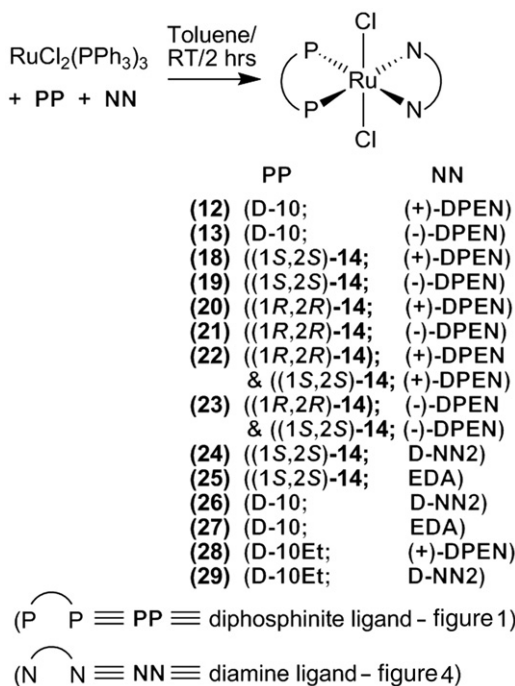
Scheme 3.   Syntheses of **12**, **13**, and **18–29**.

grown from dichloromethane/hexane and the structure obtained. The unit cell contains one inversion related pair of the enantiomers RuHCl[(1S,2S)-14]$_2$ and RuHCl[(1R,2R)-14]$_2$. The ORTEP diagram of RuHCl[(1R,2R)-14]$_2$ is shown in figure 2. The geometry about ruthenium is close to octahedral with the hydride and chloride ligands mutually *trans*. The two diphosphinite ligands occupy the four other coordination sites, but as can be seen from the ORTEP diagram, the four phosphorus atoms and ruthenium are not coplanar. The relevant angles are P1–Ru–P-4 = 176.40(3)° and P2–Ru–P3 = 158.28(3)°. The Ru–P2 and Ru–P3 distances [2.3285(7) and 2.3251(7) Å, respectively] are slightly shorter than the Ru–P1 and Ru–P4 distances [2.3729(7) and 2.3563(7) Å, respectively]. The Ru–Cl distance of 2.5520(7) Å is longer than the average Ru–Cl distance of 2.407 Å recorded in the Cambridge Crystallographic Database (4879 obs, SD 0.047 Å), most likely as a result of the *trans*-influence of the hydride ligand.

On the treatment of (*rac*)-**16** with hydrogen in iso-propanol using conditions similar to those used for the hydrogenation studies (section 2.4), a racemic mixture of the dihydride complexes RuH$_2$[(1S,2S)-14]$_2$ and RuH$_2$[(1R,2R)-14]$_2$ [(*rac*)-**17**] is formed in very good yield (scheme 2). The structure of (*rac*)-**17** shown in scheme 2 was confirmed by X-ray structure determination. Although the two hydrides are mutually *cis*, the complex retains a C_2 axis which relates the two hydrides and the two diphosphinite ligands. Again the six cyclohexane ring carbons within one diphosphinite ligand are all inequivalent and the corresponding six signals are observed in the ^{13}C NMR spectrum at 23.1, 24.0, 32.8, 32.9, 76.4, and 78.3 ppm. In the ^{31}P NMR spectrum two apparent triplet signals are observed for each symmetry-related pair of phosphorus atoms (at 151.07 and 153.05 ppm), consistent with coupling in the AA′XX′ spin system. In the
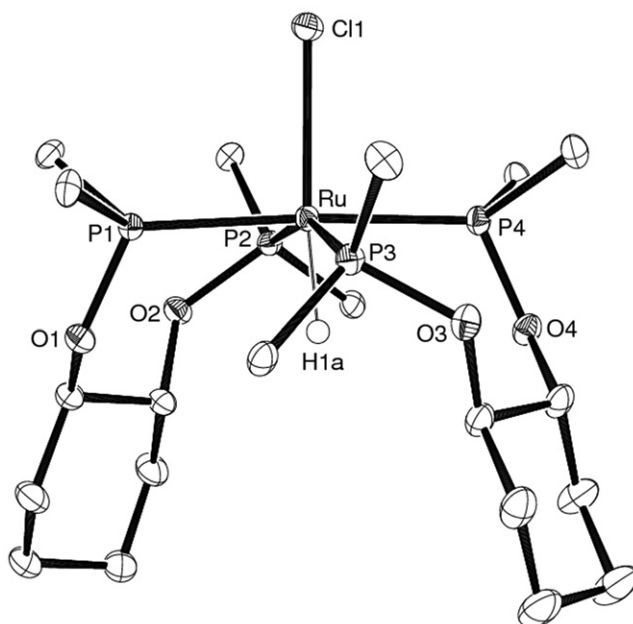
Figure 2. The inner coordination sphere of RuHCl[(1*R*,2*R*)-14]$_2$ {which co-crystallizes with the other enantiomer RuHCl[(1*S*,2*S*)-14]$_2$ in crystals of (*rac*)-**16**}.

^{1}H NMR spectrum of (*rac*)-**17** two multiplet signals that each integrate for two protons at 2.35 and 2.93 ppm are observed for the four cyclohexane CH groups, and a complex set of overlapping multiplets in the region 0.59–1.81 ppm is observed for the CH$_2$ groups. The hydride ligands are observed as a multiplet at −8.00 ppm, which collapses to a broad singlet in the ^{31}P decoupled ^{1}H NMR spectrum.

A crystal of (*rac*)-**17** suitable for X-ray structure determination was obtained from iso-propanol solution and the crystal structure determined. There is one independent molecule in centrosymmetric space group $P2_1/c$, so the unit cell contains two molecules of each enantiomer RuH$_2$[(1*S*,2*S*)-14]$_2$ and RuH$_2$[(1*R*,2*R*)-14]$_2$. The ORTEP diagram of RuH$_2$[(1*S*,2*S*)-14]$_2$ is shown in figure 3. The geometry about ruthenium is approximately octahedral with the two hydride ligands mutually *cis* and the configuration at the metal center is Λ for the RuH$_2$[(1*S*,2*S*)-14]$_2$ enantiomer. The two phosphorus atoms P1 and P4 are nearly *trans* [P1–Ru–P4 = 158.34(2)°] and the two distances Ru–P1 [2.2776(6) Å] and Ru–P4 [2.2858(7) Å] are very similar. The other phosphorus atoms, P2 and P3, are mutually *cis* [P2–Ru–P3 = 97.17(2)°] and have essentially identical distances to ruthenium [Ru–P2 = 2.3010(7) Å and Ru–P3 = 2.3010(6) Å]. These distances are both longer than the distances Ru–P1 and Ru–P4, and the differences can be ascribed to the large *trans*-influence of the hydride ligands.

2.3. Syntheses of the ruthenium diphosphinite diamine complexes 18–29 that are of general formula RuCl$_2$(diphosphinite)(diamine)

Treatment of RuCl$_2$(PPh$_3$)$_3$ with two equivalents of (1*S*,2*S*)-**14** and one equivalent of (1*R*,2*R*)-(+)-1,2-diphenylethylenediamine [(+)-DPEN] (see figure 4 for the structures of
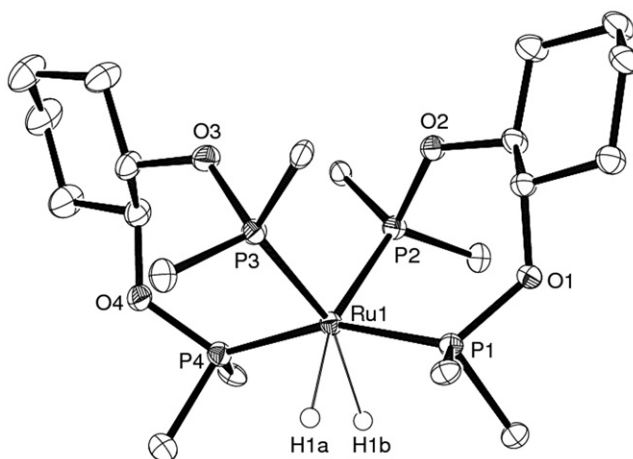
Figure 3. The inner coordination sphere of $RuH_2[(1S,2S)\text{-}14]_2$ {which co-crystallizes with the other enantiomer $RuH_2[(1R,2R)\text{-}14]_2$ in crystals of (*rac*)-**17**}.
For clarity only the *ipso* carbon atoms of the phenyl rings are shown. The thermal ellipsoids are scaled to 50% probability. Selected bond lengths (Å): Ru1–P1 2.2776(6), Ru1–P2 2.3010(7), Ru1–P3 2.3010(6), Ru1–P4 2.2858(7), Ru1–H1A 1.72(3), Ru1–H1B 1.87(3). Selected bond angles (°): P1–Ru1–P2 91.19(2), P1–Ru1–P3 101.92(2), P1–Ru1–P4 158.34(2), P2–Ru1–P3 97.17(2), P2–Ru1–P4 104.22(2), P3–Ru1–P4 91.33(2), and H1A–Ru1–H1B 60.5(12).
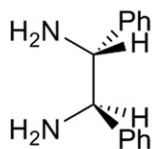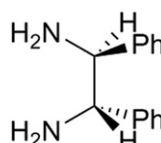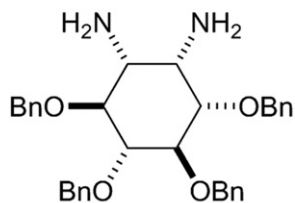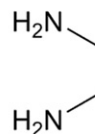
Figure 4. The diamine ligands used to synthesize compounds **18**–**29**.

the diamine ligands used to prepare the new ruthenium compounds, **18–29**) in toluene at ambient temperature produces the yellow complex RuCl$_2$[(1S,2S)-**14**][(+)-DPEN] (**18**) (scheme 3). Although the stoichiometry of complex **18** indicates that only one equivalent of the diphosphinite ligand is needed, experimentally it was found that the best yields of **18** were obtained if two equivalents were used. The other new complexes listed in scheme 3 (**19–29**) were synthesized in an analogous manner using the appropriate diphosphinite and diamine ligands. Complexes **12** and **13**, which we have reported previously [4], are also listed in scheme 3 for comparative purposes. In the ^{31}P NMR spectrum of **18**, the two phosphorus atoms of (1S,2S)-**14** appear as a sharp singlet at 148.83 ppm. This confirms that the ligands are arranged about the ruthenium, as depicted in scheme 3, with the two chloride ligands mutually *trans*. The ^{1}H and ^{13}C NMR spectra of **18** are also consistent with the geometry depicted in scheme 3, which has a C$_2$ axis bisecting the two bidentate ligands. In the ^{1}H NMR spectrum the two CH protons of the diamine ligand are a broad-structured signal at 4.42 ppm and the two CH protons of the diphosphinite ligand are similarly shaped at 4.21 ppm. The four amine protons are two broad multiplets at 3.37 and 3.50 ppm that each integrate for two protons. Cyclohexane methylene protons are observed as overlapping multiplets in the region 1.03–1.61 ppm. In the ^{13}C NMR spectrum of **18**, the three pairs of symmetry-related cyclohexane carbons appear at 23.9, 32.4, and 77.4 ppm and the two saturated carbons of (+)-DPEN appear at 63.1 ppm. RuCl$_2$[(1R,2R)-**14**][(−)-DPEN] (**21**) (see scheme 3), which can be prepared by the same method, is the enantiomer of **18** and has identical spectral properties.

RuCl$_2$[(1S,2S)-**14**][(−)-DPEN] (**19**) (scheme 3), which is a diasteriomer of **18**, has similar NMR spectral properties to **18**, but the chemical shifts are slightly different. In the ^{31}P NMR spectrum of **19**, the two phosphorus atoms appear as a sharp singlet at 147.34 ppm. In the ^{1}H NMR spectrum, the CH protons of the diamine ligand and the diphosphinite ligands are at 4.25 and 4.41 ppm, respectively. The amine protons are multiplets at 3.08 and 3.62 ppm. In the ^{13}C NMR spectrum of **19** the cyclohexane carbons appear at 23.8, 32.3, and 77.2 ppm and the two saturated carbons of (−)-**DPEN** appear at 62.8 ppm. As expected, an identical set of NMR spectra are observed for RuCl$_2$[(1R,2R)-**14**][(+)-DPEN] (**20**), which is the enantiomer of **19**.

If RuCl$_2$(PPh$_3$)$_3$ is treated with (*rac*)-**14** and (+)-DPEN, the product isolated is a mixture of equal amounts of **18** and **20** and this is denoted as compound **22** (scheme 3). As expected, the ^{1}H, ^{13}C, and ^{31}P NMR spectra of **22** show signals due to both **18** and **20**. In a similar way, the treatment of RuCl$_2$(PPh$_3$)$_3$ with (*rac*)-**14** and (−)-**DPEN** gives **23**, which is a mixture of equal amounts of **19** and **21** (scheme 3). The NMR spectra of **23** are identical to those for **22** because **18** and **21**, as well as **19** and **20**, form enantiomeric pairs.

RuCl$_2$[(1S,2S)-**14**](D-NN2) (**24**) contains the chiral diamine **D-NN2** (figure 4), which is a derivative of *myo*-inositol [21]. There is no C$_2$ axis in D-NN2, and as a result there is no C$_2$ axis in **24** either. Therefore, in the ^{13}C NMR spectrum of **24**, individual resonances are observed for each carbon of the two cyclohexane rings and for the four CH$_2$Ph methylene carbons in (1S,2S)-**14** and D-NN2. The two phosphorus atoms are also inequivalent as two doublets at 147.2 (d, $^2J_{PP} = 59.5$ Hz) and 151.4 (d, $^2J_{PP} = 59.3$ Hz) ppm. In contrast, in the related complex RuCl$_2$[(1S,2S)-**14**](EDA) (**25**), which contains the bidentate ethylenediamine ligand, the C$_2$ axis in the complex is restored and only a singlet is observed (at 147.63 ppm) for the two phosphorus atoms in

the ^{31}P NMR spectrum and three signals are observed for the cyclohexane ring atoms at 23.8, 32.0, and 77.4 ppm in the ^{13}C NMR spectrum.
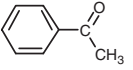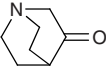
We have already reported the synthesis of the related diphosphinite complexes $RuCl_2$(D-10)[(+)-DPEN] (**12**) and $RuCl_2$(D-10)[(−)-DPEN] (**13**) (scheme 3) [4]. The diphosphinite ligand in these complexes, D-10 (see figure 1), is based on a *chiro*-inositol scaffold. In the extension of this work, we now report the syntheses of $RuCl_2$(D-10)(D-NN2) (**26**) and $RuCl_2$(D-10)(EDA) (**27**). As **24**, **26** also does not have a C_2 axis. Therefore, in the ^{31}P NMR spectrum of **26**, two resonances are observed for the inequivalent phosphorus atoms and in the ^{13}C NMR spectrum 20 separate resonances are observed for the inequivalent nonaromatic carbon atoms of the diphosphinite and diamine ligands. Less complicated NMR spectra are observed for **27** which contains ethylenediamine. In the ^{31}P NMR spectrum of **27** a single signal is observed for the two phosphorus atoms at 150.50 ppm and in the ^{1}H NMR spectrum only two methyl resonances and three CH resonances are observed for D-10, consistent with the presence of a C_2 axis that bisects the bidentate D-10 and EDA ligands.

Two complexes that contain the D-10Et ligand (figure 1), $RuCl_2$(D-10Et)[(+)-DPEN] (**28**) and $RuCl_2$(D-10Et)(D-NN2) (**29**), have also been prepared. As expected, the ^{31}P NMR spectrum of **28** contains a singlet for the two equivalent phosphorus atoms that are related by a C_2 axis. The ^{1}H and ^{13}C NMR spectra are also consistent with the presence of a C_2 axis that bisects the two bidentate ligands. Thus, in the ^{13}C NMR spectrum of **28** only one resonance is observed for the CH carbons of (+)-DPEN and three CH resonances are observed for D-10Et. Similarly, only two methyl and two methylene resonances are observed for the four ethyl substituents of this ligand. A more complex set of signals is observed in the NMR spectra for $RuCl_2$(D-10Et)(D-NN2) (**29**) reflecting the lower symmetry of this molecule. As with the other compounds that contain D-NN2 (**24** and **26**), there is no C_2 axis present in **29**. The four ethyl substituents and the four benzyl substituents are therefore all inequivalent, as are the cyclohexane ring carbons of both bidentate ligands. This is clearly seen in the ^{13}C NMR spectrum where separate resonances are observed for CH_3, CH_2O, and cyclohexane ring carbons. In the ^{31}P NMR spectrum, the two inequivalent phosphorus atoms have very similar chemical shifts giving a second order spectrum with two nearly coincident intense signals at 148.92 and 148.97 ppm.

2.4. *Investigation of the catalytic activity of the new ruthenium diphosphinite complexes in asymmetric hydrogenation reactions of the prochiral substrates acetophenone and 3-quinuclidinone*

In a previous study, we reported the results of our investigations into the catalytic activity of **11**, **12**, and **13** towards the asymmetric hydrogenation of the ketones acetophenone (to give *sec*-phenylethyl alcohol) and 3-quinuclidinone (to give 3-quinuclidinol) [4]. We now present catalytic asymmetric hydrogenation reactions of the same substrates in the presence of the new ruthenium complexes described in sections 2.2 and 2.3. Identical conditions to those in the previous study were used for the hydrogenation reactions so that direct comparisons could be made with the earlier results. The reactions were carried out in toluene/iso-propanol solution (1 : 1) with a substrate to catalyst ratio of 200 : 1, hydrogen pressure of 1000 psi, temperature of 60°C, and a time period of 3 h. As before, KO^{t}Bu (2 M equivalent *vs.* the ruthenium complex)

Table 1. Conversion (%), %ee, and configuration of the major enantiomer formed during the catalytic hydrogenation of acetophenone and 3-quinuclidinone.

Precatalyst	Acetophenone		3-Quinuclidinone	
	Conversion (%)	%ee (configuration)	Conversion (%)	%ee (configuration)
RuHCl(D-10)$_2$ (**11**)	20	2 (*R*)	97	2 (*S*)
RuHCl[(1*S*,2*S*)-14]$_2$ (**15**)	0	NA	99	10 (*R*)
RuCl$_2$(D-10)[(+)-DPEN] (**12**)	100	25 (*S*)	100	8 (*S*)
RuCl$_2$(D-10)[(−)-DPEN] (**13**)	100	24 (*R*)	100	54 (*R*)
RuCl$_2$[(1*S*,2*S*)-14][(+)-DPEN] (**18**)	100	49 (*S*)	99	38 (*S*)
RuCl$_2$(1*S*,2*S*)-14][(−)-DPEN] (**19**)	100	31 (*R*)	99	6 (*S*)
RuCl$_2$[(1*R*,2*R*)-14][(+)-DPEN] (**20**)	100	25 (*S*)	99	5 (*S*)
RuCl$_2$[(1*R*,2*R*)-14][(−)-DPEN] (**21**)	100	53 (*R*)	100	39 (*R*)
RuCl$_2$[(1*S*,2*S*)-14][(+)-DPEN] and RuCl$_2$[(1*R*,2*R*)-14][(+)-DPEN] (**22**)	100	26 (*S*)	100	23 (*S*)
RuCl$_2$[(1*S*,2*S*)-14][(−)-DPEN] and RuCl$_2$[(1*R*,2*R*)-14][(−)-DPEN] (**23**)	100	32 (*R*)	100	26 (*R*)
RuCl$_2$[(1*S*,2*S*)-14](D-NN2) (**24**)	100	61 (*S*)	99	41 (*S*)
RuCl$_2$[(1*S*,2*S*)-14](EDA) (**25**)	100	17 (*S*)	99	13 (*S*)
RuCl$_2$(D-10)(D-NN2) (**26**)	100	32 (*S*)	100	3 (*R*)
RuCl$_2$(D-10)(EDA) (**27**)	100	18 (*R*)	99	30 (*R*)
RuCl$_2$(D-10Et)[(+)-DPEN] (**28**)	100	19 (*S*)	99	4 (*S*)
RuCl$_2$(D-10Et)(D-NN2) (**29**)	100	32 (*S*)	97	27 (*R*)

Conditions: substrate: precatalyst ratio, 200: 1; hydrogen pressure, 1000 psi; KO^{t}Bu (2M *vs.* ruthenium complex); temperature, 60°C; time, 3 h; solvent, toluene/iso-propanol (1 : 1).

was added to each reaction because it has been shown that the presence of this base can significantly improve the yield of product formed in catalytic hydrogenation reactions, especially with complexes that incorporate a diamine ligand [22].

The hydrogenation results are presented in table 1 and the data previously obtained for **11**, **12**, or **13** [4] are also included for comparative purposes. The ruthenium complexes studied were selected to examine how changes to the diphosphinite and diamine ligands influence the %ee values of the products formed. The results presented in table 1 are discussed further in this context.

Compounds **11** and **15** are bis(diphosphinite) complexes of Ru(II). Whereas D-10 in **11** is based on the *chiro*-inositol backbone, (1*S*,2*S*)-**14** in **15** is based on the related, less sterically encumbered cyclohexanediol backbone (figure 1). Complex **11** does not effectively catalyze the hydrogenation of acetophenone under the conditions used and **15** showed no detectible activity at all. In contrast, both complexes catalyzed the complete hydrogenation of 3-quinuclidinone, although in both cases very little, if any, enantiomeric excess was observed in the products. A potentially complicating factor in the hydrogenation reactions involving **15** or (*rac*)-**16** was that the corresponding ruthenium dihydride complexes RuH$_2$[(1*S*,2*S*)-14]$_2$ or (*rac*)-**17** crystallized from solution in significant amounts as the reactions proceeded. Exploratory experiments in which acetophenone was subjected to the standard hydrogenation conditions in the presence of (*rac*)-**17** resulted in no hydrogenated products, and with 3-quinuclidinone only *ca* 50% conversion to hydrogenated products was observed. These results indicated that under these conditions the dihydride complexes have lower catalytic activity than the precursor chloro hydride complexes, and were therefore not

studied further. The formation of crystalline ruthenium derivatives was not observed during the hydrogenation reactions involving any of the other ruthenium complexes studied.

The remaining complexes listed in table 1 each contain one chelating diphosphinite, one chelating diamine, and two chlorides. All these complexes catalyzed the hydrogenation of both acetophenone and 3-quinuclidinone with essentially complete conversion under the conditions used. Complexes **12**, **18**, **20**, and **28** all have the same diamine ligand [(+)-DPEN] but different diphosphinite ligands. Comparison of the hydrogenation results obtained with these different catalysts indicates that replacing D-10 (which has methoxy substituents) in complex **12** with D-10Et (which has ethoxy substituents) to give complex **28** has a slightly detrimental effect on the %ee values of the products, while **20** with the less encumbered diphosphinite ligand (1*R*,2*R*)-**14** shows almost identical behavior to that observed for **12**. Compound **18** (a diastereomer of **20**) gives products with much higher %ee values (49% for acetophenone and 38% for quinuclidinone) than any of the other complexes in this set, even though the actual values are still modest. Presumably, the (1*S*,2*S*)-**14** and (+)-DPEN ligands in **18** work in concert as a "matched pair" to effect asymmetric hydrogenation of these substrates. Complexes **13**, **19**, and **21** contain (−)-DPEN. Complex **13**, which is a diastereomer of **12**, catalyzes the hydrogenation of acetophenone to give products with essentially the same %ee (but opposite stereochemistry), as obtained with **12**. However, in the hydrogenation of 3-quinuclidinone, **13** gives products with a much higher %ee (54%) compared with **12** (8%), again showing that the combination of chiral ligands is very important in determining %ee. Complexes **19** and **20** are enantiomers and, as expected, the reactions catalyzed by **19** give, within experimental error, products with the same %ee as those catalyzed by **20**, but with the dominant enantiomer having the opposite chirality. A similar situation is observed for enantiomers **18** and **21**.

The material designated **22** is an equal mixture of the diastereomers **18** and **20**, and similarly **23** is an equal mixture of the diastereomers **19** and **21**. As might be expected, the %ee values of the products obtained from **22** lie between the corresponding values obtained for reactions catalyzed by the individual complexes **18** and **20**. The relative rates at which each product enantiomer is formed by the two components **18** and **20** will be important factors in determining the %ee of the products produced by **22**. A similar situation is observed for **23** where again the %ee values of the products lie between the corresponding values obtained for reactions catalyzed by the individual complexes **19** and **21**. Each of the components of **22** form an enantiomeric pair with one of the components of **23**, that is, **18** and **21** form an enantiomeric pair, as do **19** and **20**. Accordingly, the %ee values obtained for the hydrogenation reactions of **22** and **23** are the same within experimental error, but the dominant enantiomer obtained from the hydrogenation of each substrate has the opposite chirality.

The remaining data in table 1 provides some information about the influence that the diamine ligand in the complex has on the %ee values of the products. The set of complexes **12**, **13**, **26**, and **27** all contain the same diphosphinite ligand, D-10, but have different chelating diamine ligands. For the hydrogenation of acetophenone, similar %ee's (*ca* 25%) are observed for **12** [with (+)-DPEN] and **13** [with (−)-DPEN], while the higher value of 32% ee is observed for **26** (with D-NN2) and the lower value of 18% ee is observed for **27** (with EDA). The same trend is not observed for the hydrogenation of 3-quinuclidinone, where the complexes and corresponding %ee values of the products are **12** (8%), **13** (54%), **26** (3%), and **27** (30%). In this case **13** gives the highest

value, and there is a big difference between **12** and **13**, and **26** giving the lowest value. Once again these results reinforce the importance of ligands working in concert as ''matched pairs'' to effect asymmetric hydrogenation of a particular substrate.

Comparisons of the products formed during reactions catalyzed by **18**, **19**, **24**, and **25**, which contain the (1*S*,2*S*)-**14** diphosphinite ligand but have different diamine ligands, reveal that for the hydrogenation of acetophenone the complex that contains the D-NN2 diamine ligand (**24**) again gives the highest %ee value (61%). This same complex also gives the highest %ee value (41%) of this set for the hydrogenation of 3-quinuclidinone. Unlike the situation discussed above for **12**, **13**, **26**, and **27**, for the set of complexes **18**, **19**, **24**, and **25**, the trend in increasing %ee values observed for acetophenone is essentially the same as the trend observed for 3-quinuclidinone. Of the two complexes prepared with D-10Et (**28** and **29**), the complex with the **D-NN2** diamine (**29**) gave the higher %ee values for the catalytic hydrogenation of both ketone substrates.

The following general remarks can be made about the ability of the complexes that are listed in table 1 to catalyze the asymmetric hydrogenation of acetophenone and 3-quinuclidinone. Under the conditions used, bis(diphosphinite) complexes **11** and **15** performed very poorly as asymmetric hydrogenation catalysts. Much better results were obtained with some of the mixed diphosphinite, diamine complexes. Of the complexes studied, **24** gave the highest %ee value for the hydrogenation of acetophenone (61%), while **13** (which has different diphosphinite and diamine ligands) gave the highest %ee value for the hydrogenation of 3-quinuclidinone (54%). Compared with other catalytic systems, however, both these %ee values are modest [17, 23]. There was no evidence obtained from these studies that there is an advantage in using one particular diphosphinite or diamine ligand for the production of effective catalysts. Rather, the results serve to confirm the general observation that a particular combination of ligands that works well for one substrate will not necessarily be ideal for others. This further highlights the need to extend the pool of chiral ligands that are available for the construction of asymmetric hydrogenation catalysts.

3. Experimental

3.1. *General synthetic procedures and instruments*

Manipulations of air sensitive materials were conducted using either Schlenk techniques (nitrogen atmosphere) or an Innovative Technology inert atmosphere glove box (argon atmosphere). Tetrahydrofuran, ether and toluene were distilled from sodium benzophenone ketyl under nitrogen and stored over activated 4 Å molecular sieves. Dichloromethane was distilled from calcium hydride. *n*-Hexane was purified by passage through a column of activated alumina. Triethylamine was distilled from calcium hydride and stored over potassium hydroxide. Flash column chromatography was carried out on 230–400 silica (Scharlau). ^{1}H, ^{13}C, and ^{31}P NMR spectra were obtained on a Bruker Avance 300 at 25°C operating at 300.13 (^{1}H), 75.48 (^{13}C), and 121.5 (^{31}P) MHz, respectively. Resonances are quoted in parts per million and the ^{1}H NMR is referenced to the protio-impurity in the solvent (7.25 ppm for CDCl$_3$) or TMS (0.00 ppm). ^{13}C NMR spectra were referenced to CDCl$_3$ (77.00 ppm) and ^{31}P NMR spectra to 85% orthophosphoric acid (0.00 ppm) as an external standard.

Elemental analyses were obtained from the Microanalytical Laboratory, University of Otago. FAB+ mass spectra were obtained from a VG-70SE machine. Chloro-diphenylphosphine, (*rac*)-*trans*-1,2-cyclohexanediol, (1*S*,2*S*)-*trans*-1,2-cyclohexanediol, (1*R*,2*R*)-*trans*-1,2-cyclohexanediol, (+)-DPEN, (−)-DPEN, and EDA were obtained commercially. D-7, D-10, D-NN2 [21], [RuCl$_2$(COD)]$_n$ [24, 25], and RuCl$_2$(PPh$_3$)$_3$ [26] were all prepared according to literature methods.

3.2. *General procedures and instruments employed for the hydrogenation reactions*

Hydrogenations were carried out in 12 mL glass vials equipped with a magnetic stirrer bar. The vials were filled with catalyst (0.005 mmol), substrate (1.0 mmol), KO^{t}Bu (0.01 mmol), and 1:1 toluene/iso-propanol (3 mL) for both the acetophenone and 3-quinuclidinone substrates inside an inert atmosphere glove box and then placed inside a 300 mL Parr autoclave made from Hastelloy C. In this way, several hydrogenation experiments could be carried out at the same time. The autoclave was sealed, taken outside the glovebox, and heated to 60°C using a thermostatic heating mantle. The autoclave was then flushed with hydrogen three times before being filled with hydrogen (1000 psi). After 3 h the autoclave was cooled and the pressure reduced to atmospheric pressure. The autoclave was then opened and samples of the crude reaction mixture were analyzed by GC. The GC analysis to obtain conversion and enantiomeric excess values were performed on a HP 6890 Series gas chromatography apparatus with an FID detector using a capillary Supelco GAMMA-DEX 225 (30 m × 0.25 mm × 0.25 μm) column or a SGE CYDEX-B (2 m × 0.32 mm × 0.25 μm) column. The estimated error in each %ee value is ± 5%. The GC methods that were established for the two prochiral substrates were (1) acetophenone (80°C isothermal): starting material t_R (min) 29.4; products t_R (min) *R* 33.3, *S* 34.2; (2) 3-quinuclidinone (140°C for 10 min then ramped up to 220°C at 10°C min^{-1}): starting material t_R (min) 10.8; products t_R (min) *R* 12.5, *S* 12.9.

3.3. *Preparation of a racemic mixture of (1R,2R)-1,2-trans-bis-(O-diphenylphosphino)cyclohexane [(1R,2R)-14] and (1S,2S)-1,2-trans-bis-(O-diphenylphosphino)cyclohexane [(1S,2S)-14)], [(rac)-14]*

To a solution of (*rac*)-*trans*-1,2-cyclohexanediol (1.0 g, 8.6 mmol) and pyridine (1.4 mL, 17.2 mmol) in tetrahydrofuran (15 mL), ClPPh$_2$ (3.1 mL, 17.2 mmol) was added dropwise and the solution was stirred at RT for 16 h. The solution was then transferred *via* a cannula fitted with a filter to another flask under nitrogen and tetrahydrofuran was removed under reduced pressure to yield (*rac*)-**14** as a white solid (3.75 g, 90%). ^{1}H NMR (CDCl$_3$, δ): 1.22–1.28 (m, 2H, C*H*$_2$), 1.44–1.48 (m, 2H, C*H*$_2$), 1.59–1.63 (m, 2H, C*H*$_2$), 2.02–2.06 (m, 2H, C*H*$_2$), 3.99–4.04 (m, 2H, C*H*), and 7.17–7.51 (m, 20H, *Ph*). ^{13}C{^{1}H} NMR (CDCl$_3$, δ): 22.6 (*C*H$_2$), 31.2 (*C*H$_2$), 81.2 (*C*H), and 128.0–130.5 (multiple signals, *Ph*). ^{31}P{^{1}H} NMR (CDCl$_3$, δ): 107.30.

3.4. *Preparation of (1S,2S)-1,2-trans-bis-(O-diphenylphosphino)cyclohexane [(1S,2S)-14]*

The same procedure that was used for synthesis of (*rac*)-**14** was followed except that (1*S*,2*S*)-*trans*-1,2-cyclohexanediol was used instead of *rac*-*trans*-1,2-cyclohexanediol. The ^{1}H, ^{13}C, and ^{31}P NMR spectra were identical to those obtained for (*rac*)-**14**.

3.5. *Preparation of (1R,2R)-1,2-trans-bis-(O-diphenylphosphino)cyclohexane [(1R,2R)-14]*

The same procedure that was used for the synthesis of (*rac*)-**14** was followed except that (1*R*,2*R*)-*trans*-1,2-cyclohexanediol was used instead of *rac-trans*-1,2-cyclohexanediol. The ^{1}H, ^{13}C, and ^{31}P NMR spectra were identical to those obtained for (*rac*)-**14**.

3.6. *Preparation of 1D-3,4-bis(O-diphenylphosphino)-1,2,5,6-tetra-O-ethyl-chiro-inositol (D-10Et)*

The ligand D-10Et was synthesized from D-**7** following the same procedure that was used for the synthesis of the corresponding tetramethyl ligand D-10 [4] except that ethyl bromide was substituted for methyl iodide in the first step (scheme 1). Pure D-10Et was obtained as a white solid in 60% overall yield. Anal. Calcd for $C_{38}H_{46}O_6P_2$: C, 69.08; H, 7.02. Found: C, 68.86; H, 6.88. ^{1}H NMR (CDCl$_3$, δ): 0.64 (apparent t, 6H, CH_3), 1.18 (apparent t, 6H, CH_3), 2.72–4.93 (m, 14H, CH, CH_2), 6.94–7.83 (m, 20H, *Ph*). ^{13}C{^{1}H} NMR (CDCl$_3$, δ): 14.7 (*C*H$_3$), 15.4 (*C*H$_3$), 66.9 (*C*H$_2$CH$_3$), 67.2 (*C*H$_2$CH$_3$), 76.1 (*C*H), 77.9 (*C*H), 78.9 (*C*H), 127.3–133.0 (multiple signals, *Ph*). ^{31}P{^{1}H} NMR (CDCl$_3$, δ): 109.47 (s).

3.7. *Preparation of RuHCl[(1S,2S)-14]₂ (15)*

Compound (1*S*,2*S*)-**14** (0.090 g, 0.19 mmol), triethylamine (0.06 mL, 0.4 mmol), and [RuCl$_2$(COD)]$_n$ (0.030 g, 0.10 mmol) in toluene (30 mL) were heated under reflux for 6 h. The toluene was removed under reduced pressure and the resulting residue was dissolved in a minimum of dichloromethane and purified by column chromatography on basic alumina using dichloromethane as the eluent. The orange/yellow band was collected and the dichloromethane was removed under reduced pressure. The resulting residue was recrystallized from dichloromethane/*n*-hexane to give pure **15** as an orange/yellow solid (0.036 g, 34%). MS (*m/z*): Calcd for $C_{60}H_{61}{}^{35}ClO_4P_4{}^{102}Ru$ (M$^+$) 1106.2252 (*m/z*). Found: 1106.2269. ^{1}H NMR (CDCl$_3$, δ): −16.38 (m, 1H, RuH), 0.80–2.35 (m, 16H, CH_2), 3.76 (m, 2H, CH), 5.10 (m, 2H, CH), and 6.55–7.72 (m, 40H, *Ph*). ^{13}C NMR{^{1}H} (CDCl$_3$, δ): 24.4 (*C*H$_2$), 24.5 (*C*H$_2$), 32.3 (*C*H$_2$), 33.0 (*C*H$_2$), 75.7 (*C*H), 78.9 (*C*H), and 125.6–147.3 (multiple signals, *Ph*). ^{31}P{^{1}H} NMR (CDCl$_3$, δ): 118.13 (apparent t, lower intensity signals at 117.76 and 118.50), 147.26 (apparent t, lower intensity signals at 146.89 and 147.63).

3.8. *Preparation of a racemic mixture of RuHCl[(1S,2S)-14]₂ and RuHCl[(1R,2R)-14]₂ [(rac)-16]*

Compound (*rac*)-**14** (7.507 g, 15.50 mmol), triethylamine (20 mL, 144 mmol), and [RuCl$_2$(COD)]$_n$ (1.61 g, 5.70 mmol) in toluene (50 mL) were heated under reflux for 12 h giving a yellow/orange solid suspended in solution. The solid was filtered and washed with hexane (3 mL × 5 mL) to give pure (*rac*)-**16** as a yellow/orange solid (5.658 g, 90%). Anal. Calcd for $C_{60}H_{61}ClO_4P_4Ru$: C, 65.13; H, 5.56. Found: C, 65.12; H, 5.79. The ^{1}H, ^{13}C and ^{31}P NMR spectra were identical to those obtained for **15**.

3.9. *Preparation of a racemic mixture of RuH$_2$[(1S,2S)-14]$_2$ and RuH$_2$[(1R,2R)-14]$_2$ [(rac)-17]*

Compound (*rac*)-**16** (0.500 g, 0.452 mmol) and KO^{t}Bu (0.067 g, 0.60 mmol) were added to degassed iso-propanol (32 mL) and placed in an autoclave inside a drybox (argon atmosphere). The autoclave was then sealed, removed from the drybox and heated at 60°C under 1000 psi of hydrogen for 16 h. On cooling and release of the pressure, pure (*rac*)-**17** was obtained from the solution by filtration as a cream/yellow microcrystalline solid (0.45 g, 93%). Anal. Calcd for C$_{60}$H$_{62}$O$_4$P$_4$Ru: C, 67.22; H, 5.83. Found: C, 67.00; H, 5.84. MS (*m/z*): Calcd for C$_{60}$H$_{61}$O$_4$P$_4$^{102}Ru (M − H)$^+$ 1071.25639 *m/z*. Found: 1071.25820. ^{1}H NMR (CDCl$_3$, δ): −8.00 (m, 2H, RuH), 0.59–1.81 (m, 16H, CH_2), 2.35 (m, 2H, CH), 2.93 (m, 2H, CH), and 6.88–7.97 (m, 40H, *Ph*). ^{13}C NMR{^{1}H} (CDCl$_3$, δ): 23.1 (*C*H$_2$), 24.0 (*C*H$_2$), 32.8 (*C*H$_2$), 32.9 (*C*H$_2$), 76.4 (*C*H), 78.3 (*C*H), and 126.5–131.6 (multiple signals, *Ph*). ^{31}P{^{1}H} NMR (CDCl$_3$, δ): 151.07 (apparent t, lower intensity signals at 150.84 and 151.31), 153.05 (apparent t, lower intensity signals at 152.82 and 153.30).

3.10. *Preparation of RuCl$_2$[(+)-DPEN][(1S,2S)-14] (18)*

Compound (1*S*,2*S*)-**14** (0.17 g, 0.34 mmol) and RuCl$_2$(PPh$_3$)$_3$ (0.16 g, 0.17 mmol) were added to toluene (20 mL) under nitrogen and stirred at 18°C for 1 h. (+)-DPEN (0.037 g, 0.17 mmol) was then added and the mixture was stirred for an additional hour at the same temperature. The toluene was removed under reduced pressure and the crude solid dissolved in a minimum of dichloromethane and purified using column chromatography. A bright yellow band was removed from the column using dichloromethane as the eluent. The dichloromethane was removed under reduced pressure and the residue was recrystallized from dichloromethane/*n*-hexane to give pure **18** as a yellow crystalline solid (0.045 g, 46%). MS (*m/z*): Calcd for C$_{44}$H$_{46}$^{35}Cl$_2$N$_2$O$_2$P$_2$^{102}Ru (M$^+$) 868.14551 *m/z*. Found: 868.14396. ^{1}H NMR (CDCl$_3$, δ): 1.03–1.61 (m, 8H, CH_2), 3.37 (m, 2H, NH_2), 3.50 (m, 2H, NH_2), 4.21 (m, 2H, CH diphosphinite), 4.42 (m, 2H, CH diamine), 6.99–7.80 (m, 30H, *Ph*). ^{13}C{^{1}H} NMR (CDCl$_3$, δ): 23.9 (*C*H$_2$), 32.4 (*C*H$_2$), 63.1 (*C*H diamine), 77.4 (*C*H diphosphinite), and 127.0–133.9 (multiple signals, *Ph*). ^{31}P{^{1}H} NMR (CDCl$_3$, δ): 148.83 (s).

3.11. *Preparation of RuCl$_2$[(−)-DPEN][(1S,2S)-14] (19)*

The same procedure that was used for the synthesis of **18** was followed except that (−)-DPEN was used instead of (+)-DPEN. After recrystallization from diethylether/ *n*-hexane, pure **19** was obtained as yellow crystals in 20% yield. MS (*m/z*): Calcd for C$_{44}$H$_{46}$^{35}Cl$_2$N$_2$O$_2$P$_2$^{102}Ru (M$^+$) 868.14551 *m/z*. Found: 868.14618. ^{1}H NMR (CDCl$_3$, δ): 0.88–1.64 (m, 8H, CH_2), 3.08 (m, 2H, NH_2), 3.62 (m, 2H, NH_2), 4.25 (m, 2H, CH diphosphinite), 4.41 (m, 2H, CH diamine), 6.98–7.77 (m, 30H, *Ph*). ^{13}C{^{1}H} NMR (CDCl$_3$, δ): 23.8 (*C*H$_2$), 32.3 (*C*H$_2$), 62.8 (*C*H diamine), 77.2 (*C*H diphosphinite), and 127.0–133.6 (multiple signals, *Ph*). ^{31}P{^{1}H} NMR (CDCl$_3$, δ): 147.34 (s).

3.12. *Preparation of RuCl$_2$[(+)-DPEN][(1R,2R)-14] (20)*

The same procedure used for the synthesis of **18** was followed except that (1*R*,2*R*)-**14** was used instead of (1*S*,2*S*)-**14**. After recrystallization from diethylether/*n*-hexane, pure

20 was obtained as yellow crystals in 70% yield. MS (m/z): Calcd for $C_{44}H_{46}{}^{35}Cl_2N_2O_2P_2{}^{102}Ru$ (M$^+$) 868.14551 m/z. Found: 868.14365. The ^1H, ^{13}C, and ^{31}P NMR spectra were identical to those obtained for **19**.

3.13. *Preparation of RuCl₂[(−)-DPEN][(1R,2R)-14] (21)*

The same procedure used for the synthesis of **18** was followed except that (1R,2R)-**14** was used instead of (1S,2S)-**14** and (−)-DPEN was used instead of (+)-DPEN. After recrystallization from diethylether/n-hexane, pure **21** was obtained as yellow crystals in 60% yield. Anal. Calcd for $C_{44}H_{46}Cl_2N_2O_2P_2Ru$: C, 60.83; H, 5.34; N, 3.22. Found: C, 61.12; H, 5.47; N, 3.21. MS (m/z): Calcd for $C_{44}H_{46}{}^{35}Cl_2N_2O_2P_2{}^{102}Ru$ (M$^+$) 868.14551 m/z. Found: 868.14485. The ^1H, ^{13}C, and ^{31}P NMR spectra were identical to those obtained for **18**.

3.14. *Preparation of RuCl₂[(+)-DPEN][(rac)-14] (22)*

The same procedure used for the synthesis of **18** was followed except that (rac)-**14** was used instead of (1S,2S)-**14**. After recrystallization from diethylether/n-hexane, **22** was obtained as yellow crystals in 41% yield. Anal. Calcd for $C_{44}H_{46}Cl_2N_2O_2P_2Ru$: C, 60.83; H, 5.34; N, 3.22. Found: C, 60.74; H, 5.60; N, 3.11%. MS (m/z): Calcd for $C_{44}H_{46}{}^{35}Cl_2N_2O_2P_2{}^{102}Ru$ (M$^+$) 868.14551 m/z. Found: 868.14491. The ^1H, ^{13}C, and ^{31}P NMR spectra appeared as a 1:1 overlap of the spectra obtained for **18** and **20**.

3.15. *Preparation of RuCl₂[(−)-DPEN][(rac)-14] (23)*

The same procedure used for the synthesis of **18** was followed except that (rac)-**14** was used instead of (1S,2S)-**14** and (−)-DPEN was used instead of (+)-**DPEN**. After recrystallization from diethylether/n-hexane, pure **23** was obtained as yellow crystals in 60% yield. Anal. Calcd for $C_{44}H_{46}Cl_2N_2O_2P_2Ru$: C, 60.83; H, 5.34; N, 3.22. Found: C, 60.74; H, 5.73; N, 3.19%. MS (m/z): Calcd for $C_{44}H_{46}{}^{35}Cl_2N_2O_2P_2{}^{102}Ru$ (M$^+$) 868.14551 m/z. Found: 868.14402. The ^1H, ^{13}C, and ^{31}P NMR spectra were identical to those obtained for **22**.

3.16. *Preparation of RuCl₂(D-NN2)[(1S,2S)-14] (24)*

The same procedure used for the synthesis of **18** was followed except that D-NN2 was used instead of (+)-DPEN. After recrystallization from diethylether/n-hexane, pure **24** was obtained as yellow crystals in 85% yield. Anal. Calcd for $C_{64}H_{68}Cl_2N_2O_6P_2Ru$: C, 64.32; H, 5.73; N, 2.34. Found: C, 65.00; H, 6.09; N, 2.32%. MS (m/z): Calcd for $C_{64}H_{68}{}^{35}Cl_2N_2O_6P_2{}^{102}Ru$ (M$^+$) 1194.29732 m/z. Found: 1194.29933. ^1H NMR (CDCl₃, δ): 0.88–1.88 (m, 8H, CH_2), 2.75–4.52 (m, 12H, CH diphosphinite, CH diamine, NH_2), 4.69–4.92 (m, 8H, CH_2Ph), and 7.06–8.00 (m, 40H, Ph). $^{13}C\{^1H\}$ NMR (CDCl₃, δ): 23.7 (CH_2), 23.8 (CH_2), 32.3 (CH_2), 32.4 (CH_2), 54.4 (CH diamine), 54.9 (CH diamine), 72.8 (CH_2), 74.4 (CH_2), 75.5 (CH_2), 76.0 (CH_2), 76.2 (CH), 76.4 (CH), 77.9 (CH), 78.3 (CH), 81.5 (CH), 85.0 (CH), and 127.4–137.3 (multiple signals, Ph). $^{31}P\{^1H\}$ NMR (CDCl₃, δ): 147.2 (d, $^2J_{PP} = 59.5\,Hz$), 151.4 (d, $^2J_{PP} = 59.3\,Hz$).

3.17. *Preparation of RuCl$_2$(EDA)[(1S,2S)-14] (25)*

The same procedure used for the synthesis of **18** was followed except that **EDA** was used instead of (+)-DPEN. After recrystallization from diethylether/*n*-hexane, pure **25** was obtained as yellow crystals in 24% yield. Anal. Calcd for C$_{32}$H$_{38}$Cl$_2$N$_2$O$_2$P$_2$Ru · 0.5CH$_2$Cl$_2$: C, 51.43; H, 5.18; N, 3.69. Found: C, 51.03; H, 5.12; N, 2.99. ^{1}H NMR (CDCl$_3$, δ): 0.85–1.70 (m, 8H, C*H$_2$*), 2.73 (broad s, 2H, N*H$_2$*), 2.93 (broad s, 6H, C*H$_2$* diamine and N*H$_2$*), 4.20 (s, 2H, C*H* diphosphinite), and 7.18–7.73 (m, 20H, *Ph*). ^{13}C{^{1}H} NMR (CDCl$_3$, δ): 23.8 (*C*H$_2$), 32.0 (*C*H$_2$), 42.5 (*C*H$_2$ diamine), 77.4 (*C*H, diphosphinite), and 127.2–135.7 (multiple signals, *Ph*). ^{31}P{^{1}H} NMR (CDCl$_3$, δ): 147.63 (s).

3.18. *Preparation of RuCl$_2$(D-NN2)(D-10) (26)*

The same procedure used for the synthesis of **18** was followed except that D-10 was used instead of (1*S*,2*S*)-**14** and D-NN2 was used instead of (+)-DPEN. After recrystallization from diethylether/*n*-hexane, pure **26** was obtained as yellow crystals in 77% yield. Anal. Calcd for C$_{68}$H$_{76}$Cl$_2$N$_2$O$_{10}$P$_2$Ru: C, 62.10; H, 5.82; N, 2.13. Found: C, 61.87; H, 5.91; N, 2.18%. MS (*m/z*): Calcd for C$_{68}$H$_{76}$^{35}Cl$_2$N$_2$O$_{10}$P$_2$^{102}Ru (M$^+$) 1314.33958 *m/z*. Found: 1314.34018. ^{1}H NMR (CDCl$_3$, δ): 2.60–3.00 (m, 4H, N*H$_2$*), 3.09 (s, 3H, C*H$_3$*), 3.27 (s, 3H, C*H$_3$*), 3.38 (s, 3H, C*H$_3$*), 3.41 (s, 3H, C*H$_3$*), 3.20–3.75 (m, 8H), 4.40–5.10 (m, 12H), and 7.17–7.81 (m, 40H, *Ph*). ^{13}C{^{1}H} NMR (CDCl$_3$, δ): 53.3 (*C*H diamine), 55.3 (*C*H diamine), 58.9 (*C*H$_3$), 59.0 (*C*H$_3$), 59.7 (*C*H$_3$), 59.8 (*C*H$_3$), 71.9 (*C*H$_2$), 74.6 (*C*H$_2$), 75.3 (*C*H$_2$), 75.8 (*C*H$_2$), 76.2 (*C*H), 76.3 (*C*H), 76.9 (*C*H), 77.2 (*C*H, 2 overlapping signals), 78.2 (*C*H), 80.7 (*C*H, 2 overlapping signals), 81.2 (*C*H), 84.8 (*C*H), and 127.1–138.6 (multiple signals, *Ph*). ^{31}P{^{1}H} NMR (CDCl$_3$, δ): 149.73 (s, weak), 150.23 (s, strong), 150.31 (s, strong), and 150.82 (s, weak) (second-order spectrum).

3.19. *Preparation of RuCl$_2$(EDA)(D-10) (27)*

The same procedure used for the synthesis of **18** was followed except that D-10 was used instead of (1*S*,2*S*)-**14** and EDA was used instead of (+)-DPEN. After recrystallization from diethylether/*n*-hexane, pure **27** was obtained as yellow crystals in 24% yield. Anal. Calcd for C$_{36}$H$_{46}$Cl$_2$N$_2$O$_6$P$_2$Ru: C, 51.68; H, 5.54; N, 3.35. Found: C, 51.82; H, 5.52; N, 3.25%. MS (*m/z*): Calcd for C$_{36}$H$_{46}$^{35}Cl$_2$N$_2$O$_6$P$_2$^{102}Ru (M$^+$) 836.12517 *m/z*. Found: 836.12438. ^{1}H NMR (CDCl$_3$, δ): 2.64 (m, 2H, N*H$_2$*), 2.76 (m, 2H, N*H$_2$*), 2.90 (s, 4H, C*H$_2$*), 3.13 (s, 6H, OC*H$_3$*), 3.37 (s, 6H, OC*H$_3$*), 3.41 (m, 2H, C*H*), 3.61 (m, 2H, C*H*), 4.73 (m, 2H, C*H*), and 7.16–7.77 (m, 20H, *Ph*). ^{13}C{^{1}H} NMR (CDCl$_3$, δ): 42.8 (*C*H$_2$), 59.0 (*C*H$_3$), 59.8 (*C*H$_3$), 76.3 (*C*H), 77.2 (*C*H), 80.7 (*C*H), and 127.4–133.8 (multiple signals, *Ph*). ^{31}P{^{1}H} NMR (CDCl$_3$, δ): 150.50 (s).

3.20. *Preparation of RuCl$_2$((+)-DPEN)(D-10Et) (28)*

The same procedure used for the synthesis of **18** was followed except that D-10Et was used instead of (1*S*,2*S*)-**14**. After recrystallization from diethylether/*n*-hexane, pure **28** was obtained as yellow crystals in 39% yield. Anal. Calcd for C$_{52}$H$_{62}$Cl$_2$N$_2$O$_6$P$_2$Ru: C, 59.77; H, 5.98; N, 2.68. Found: C, 59.64; H, 5.98; N, 2.67%. MS (*m/z*): Calcd for

$C_{52}H_{62}{}^{35}Cl_2N_2O_6P_2{}^{102}Ru$ (M$^+$) 1044.25037 m/z. Found: 1044.24924. ^{1}H NMR (CDCl$_3$, δ): 0.83 (apparent t, 6H, CH_3), 1.18 (apparent t, 6H, CH_3), 2.94 (m, 2H, NH_2), 3.30–3.80 (m, 8H, CH_2), 3.50 (m, 2H, CH diphosphinite), 3.55 (m, 2H, NH_2), 3.63 (m, 2H, CH diphosphinite), 4.39 (m, 2H, CH, diamine), 4.82 (m, 2H, CH, diphosphinite), and 6.93–7.80 (m, 30H, Ph). ^{13}C{^{1}H} NMR (CDCl$_3$, δ): 15.4 (CH$_3$), 15.8 (CH$_3$), 62.9 (CH diamine), 66.7 (CH$_2$), 66.9 (CH$_2$), 76.1 (CH diphosphinite), 77.2 (CH diphosphinite), 79.1 (CH diphosphinite), and 126.9–133.6 (multiple signals, Ph). ^{31}P{^{1}H} NMR (CDCl$_3$, δ): 149.08 (s).

3.21. *Preparation of RuCl$_2$(D-NN2)(D-10Et) (29)*

The same procedure used for the synthesis of **18** was followed except that D-10Et was used instead of (1S,2S)-**14** and D-NN2 was used instead of (+)-DPEN. After recrystallization from diethylether/n-hexane, pure **29** was obtained as yellow crystals in 42% yield. Anal. Calcd for $C_{72}H_{84}Cl_2N_2O_{10}P_2Ru \cdot C_4H_{10}O$: C, 63.15; H, 6.55; N, 1.94. Found: C, 63.84; H, 6.34; N, 1.79%. MS (m/z): Calcd for $C_{72}H_{84}{}^{35}Cl_2N_2O_{10}P_2{}^{102}Ru$ (M$^+$) 1370.40218 m/z. Found: 1370.40210. ^{1}H NMR (CDCl$_3$, δ): 0.71 (apparent t, 3H, CH_3), 0.96 (apparent t, 3H, CH_3), 1.11 (apparent t, 3H, CH_3), 1.18 (apparent t, 3H, CH_3), 2.57–3.80 (m, 20H), 4.15–5.20 (m, 12H), 7.03–7.75 (m, 40H, Ph). ^{13}C{^{1}H} NMR (CDCl$_3$, δ): 15.2 (CH$_3$), 15.6 (CH$_3$), 15.7 (CH$_3$), 15.8 (CH$_3$), 53.2 (CH diamine), 55.5 (CH diamine), 66.8 (2 overlapping signals, CH$_2$CH$_3$), 67.0 (two overlapping signals, CH$_2$CH$_3$), 71.9 (CH$_2$Ph), 74.7 (CH$_2$Ph), 75.3 (CH$_2$Ph), 75.8 (CH$_2$Ph), 76.1 (CH), 76.6 (CH), 77.0 (CH), 77.2 (CH), 77.8 (CH), 78.3 (CH), 79.2 (CH, 2 overlapping signals), 81.9 (CH), 84.8 (CH), and 127.1–133.9 (multiple signals, Ph). ^{31}P{^{1}H} NMR (CDCl$_3$, δ): 148.92 and 148.97 (part of a second-order spectrum).

3.22. *X-ray crystal structure determination of (rac)-16 (a racemic mixture of RuHCl[(1S,2S)-14]$_2$ and RuHCl[(1R,2R)-14]$_2$)*

A suitable crystal of (*rac*)-**16** was isolated from dichloromethane/hexane. X-ray data were collected on a Siemens SMART CCD diffractometer using monochromated graphite Mo-Kα ($\lambda = 0.71073$ Å). Data collection method: ω-scan, range 0.8°. Data reduction and cell determination were carried out with SAINT and XPREP(SMART) programs [27]. Absorption corrections were applied using SADABS [28]. The structures were determined and refined using SHELXS-97 and SHELXL-97 program packages [29]. All non-H atoms were refined with anisotropic thermal parameters. The crystal contains 2.5 molecules of dichloromethane per molecule of complex. The dichloromethane molecules are disordered and their hydrogens have not been included. All other hydrogens were constrained to their expected geometries (C–H 0.95, and 0.99 Å) and refined with U_{iso} 1.2 or 1.5 times the U_{eq} of their parent atom. The unit cell contains one pair of enantiomers, but only RuHCl[(1R,2R)-14]$_2$ is depicted in figure 2.

Crystal data for $C_{60}H_{61}ClO_4P_4Ru \cdot 2.5(CH_2Cl_2)$ [(*rac*)-**16**]. M = 1318.8, triclinic, $P1$, $a = 12.8472(1)$ Å, $b = 15.4271(2)$ Å, $c = 17.7810(2)$ Å, $\alpha = 98.442(1)°$, $\beta = 110.008(1)°$, $\gamma = 106.490(1)°$, $V = 3056.63(6)$ Å^3, $Z = 2$, $D_x = 1.433$ mg m^{-3}, $\mu = 0.670$ mm^{-1}, $T = 83(2)$ K, measured 29,558 reflections (12,290 unique) in θ range 1.8–26.3°. $R_{int} = 0.018$. Final R indices [for 10,674 reflections with $I > 2\sigma(I)$] $R_1 = 0.043$, $wR_2 = 0.115$.

3.23. *X-ray crystal structure determination of (rac)-17 (a racemic mixture of RuH₂[(1S,2S)-14]₂ and RuH₂[(1R,2R)-14]₂)*

A suitable crystal of (*rac*)-**17** was isolated from iso-propanol and analyzed as for (*rac*)-**16**. The unit cell contains two molecules of each enantiomer, with only one, $RuH_2[(1S,2S)-14]_2$, depicted in figure 3. Crystal data for $C_{60}H_{62}O_4P_4Ru$ [(*rac*)-**17**]. $M = 1072.05$, monoclinic, $P2_1/c$, $a = 12.3274(15)$ Å, $b = 14.7526(18)$ Å, $c = 29.393(3)$ Å, $b = 95.409(2)°$, $V = 5321.6(11)$ Å^3, $Z = 4$, $D_x = 1.338 \, \mathrm{mg \, m^{-3}}$, $\mu = 0.461 \, \mathrm{mm^{-1}}$, $T = 113(2)$ K, measured 37174 reflections (10986 unique) in θ range 2.1–26.5°. $R_{int} = 0.050$. Final R indices [for 8368 reflections with $I > 2\sigma(I)$] $R_1 = 0.034$, $wR_2 = 0.074$.

Supplementary material

Crystallographic data (excluding structure factors) for (*rac*)-**16** and (*rac*)-**17** have been deposited with the Cambridge Crystallographic Data Centre as supplementary publication numbers CCDC 730333 and CCDC 730334, respectively. Copies of this information can be obtained free of charge from the Director, CCDC, 12 Union Road, Cambridge, CB2 1EZ, UK (Fax: +44-1223-336-033; Email: deposit@ccdc.cam.ac.uk or www: http://www.ccdc.cam.ac.uk).

Acknowledgements

References

[1] (a) W.S. Knowles, R. Noyori. *Acc. Chem. Res.*, **40**, 1238 (2007); (b) W.S. Knowles. *Angew. Chem. Int. Ed.*, **41**, 1998 (2002); (c) R. Noyori. *Angew. Chem. Int. Ed.*, **41**, 2008 (2002); (d) K.B. Sharpless. *Angew. Chem. Int. Ed.*, **41**, 2024 (2002).

[2] (a) W. Zhang, Y. Chi, X. Zhang. *Acc. Chem. Res.*, **40**, 1278 (2007); (b) X. Zhang. *Tetrahedron: Asymmetry*, **15**, 2099 (2004).

[3] T.T.-L. Au-Yeung, A.S.C. Chan. *Coord. Chem. Rev.*, **248**, 2151 (2004).

[4] A. Falshaw, G.J. Gainsford, C. Lensink, A.T. Slade, L.J. Wright. *Polyhedron*, **26**, 329 (2007).

[5] S. Castillon, C. Claver, Y. Diaz. *Chem. Soc. Rev.*, **34(8)**, 702 (2005).

[6] R. Selke. *J. Organomet. Chem.*, **370**, 249 (1989).

[7] T.V. RajanBabu, T.A. Ayers, G.A. Halliday, K.K. You, J.C. Calabrese. *J. Org. Chem.*, **62**, 6012 (1997).

[8] R. Selke. In *Asymmetric Catalysis on Industrial Scale*, H.U. Blaser, E. Schmidt (Eds.), p. 39, Wiley-VCH, Weinheim (2004).

[9] M. Diéguez, O. Pàmies, C. Claver. *Chem. Rev.*, **104**, 3189 (2004).

[10] M. Diéguez, O. Pàmies, A. Ruiz, Y. Díaz, S. Castillón, C. Claver. *Coord. Chem. Rev.*, **248**, 2165 (2004).

[11] B. Saha, T.V. RajanBabu. *Org. Lett.*, **8**, 4657 (2006).

[12] V.N. Azev, M. d'Alarcao. *J. Org. Chem.*, **69**, 4839 (2004).

[13] (a) H. Doucet, T. Ohkuma, K. Murata, T. Yokozawa, M. Kozawa, E. Katayama, A.F. England, T. Ikariya, R. Noyori. *Angew. Chem. Int. Ed.*, **37**, 1703 (1998); (b) Y. Xu, N.W. Alcock, G.J. Clarkson, G. Docherty, G. Woodward, M. Wills. *Org. Lett.*, **6**, 4105 (2004).

[14] D.S. Clyne, Y.C. Mermet-Bouvier, N. Nomura, T.V. RajanBabu. *J. Org. Chem.*, **64**, 7601 (1999).

[15] T.V. RajanBabu, B. Radetich, K.K. You, T.A. Ayers, A.L. Casalnuovo, J.C. Calabrese. *J. Org. Chem.*, **64**, 3429 (1999).

[16] (a) E. Guimeta, J. Paradab, M. Diéguez, A. Ruiz, C. Claver. *Appl. Catal., A*, **282**, 215 (2005); (b) A. Fuerte, M. Iglesias, F. Sánchez. *J. Organomet. Chem.*, **588**, 186 (1999); (c) T.V. RajanBabu, T.A. Ayers. *Tetrahedron Lett.*, **35**, 4295 (1994).

[17] S.E. Clapham, A. Hadzovic, R.H. Morris. *Coord. Chem. Rev.*, **248**, 2201 (2004).

[18] C. Sui-Seng, A. Hadzovic, A.J. Lough, R.H. Morris. *Dalton Trans.*, 2536 (2007).

[19] (a) T. Ikariya, Y. Ishii, H. Kawano, T. Arai, M. Saburi, S. Yoshikawa, S. Akutagawa. *J. Chem. Soc., Chem. Commun.*, 922 (1985); (b) V. Ratovelomanana-Vidal, J. Genet. *J. Organomet. Chem.*, **567**, 163 (1998); (c) T. Ohta, H. Takaya, R. Noyori. *Inorg. Chem.*, **27**, 566 (1988); (d) C.C. Lu, J.C. Peters. *J. Am. Chem. Soc.*, **126**, 15818 (2004).

[20] M. Schlaf, A.J. Lough, R.H. Morris. *Organometallics*, **16**, 1253 (1997).

[21] V.N. Azev, M. d'Alarcao. *J. Org. Chem.*, **69**, 4839 (2004).

[22] C.A. Sandoval, T. Ohkuna, K. Muniz, R. Noyori. *J. Am. Chem. Soc.*, **125**, 13490 (2003).

[23] C.A. Sandoval, Y. Yamaguchi, T. Ohkuma, K. Kato, R. Noyori. *Magn. Reson. Chem.*, **44**, 66 (2006).

[24] M.A. Bennett, G. Wilkinson. *Chem. Ind.*, 1516 (1959).

[25] J. Chatt, L.M. Venzanzi. *J. Chem. Soc.*, 4735 (1957).

[26] L.A. Ortiz-Frade, L. Ruiz-Ramirez, I. Gonzalez, A. Marin-Becerra, M. Alcarazo, J.G. Alvarado-Rodriguez, R. Moreno-Esparza. *Inorg. Chem.*, **42**, 1825 (2003).

[27] Siemens, *SMART and SAINT, (Versions 4.0),*. Siemens Analytical X-ray Instruments Inc., Madison, Wisconsin, USA (1996).

[28] G.M. Sheldrick. *SADABS. Program for Semi-empirical Absorption Correction*, University of Göttingen, Göttingen, Germany (1996).

[29] G.M. Sheldrick. *SHELXL97 and SHELXS97. Programs for Crystal Structure Determination and Refinement*, University of Göttingen, Göttingen, Germany (1997).